Michael Ogonnaya Ogbuatu[1], Kenechukwu Conrad Enenebeaku[1], Chritogonus Oudney Akalezi[1], Stanley Toochukwu Ekwueme[2], Ali Billar[1], Ijeoma Akunna Duru[1], TochukwuIfeanyi Nwakile[1]

[1]Department of Chemistry, Federal University of Technology, Owerri, Nigeria, [2]Department of Petroleum Engineering, Federal University of Technology, Owerri, Nigeria

Scientific paper
ISSN 0351-9465, E-ISSN 2466-2585
https://doi.org/10.62638/ZasMat1296

Zastita Materijala 66 ( )
(2025)

Process simulation and optimisation of hydrogen production from natural gas via steam methane reforming: Aspen hysys simulation investigation

ABSTRACT

The growing demand for hydrogen in the energy sector necessitates enhanced methods for its production. Presently, natural gas remains the primary feedstock for commercial hydrogen production. While green hydrogen production from renewable sources is gaining attention, it still faces economic challenges compared to fossil-derived hydrogen. This study focused on simulating hydrogen production from natural gas using the steam methane reforming (SMR) process. The simulation employed Abbas et al (2017) kinetics over 18 wt. % NiO/a-Al_2O_3catalyst within Aspen HYSYS V11 software and utilized the Peng Robinson fluid property package. Sensitivity analyses were conducted, emphasizing parameters such as temperature, pressure, molar flow rate of steam, and reactor volume. The goal was to optimize various process outcomes, including methane conversion, hydrogen selectivity and yield, methane selectivity, CO selectivity and yield, CO_2 selectivity and yield, H_2/CO ratio, and hydrogen production. The results indicated that methane conversion and selectivities for hydrogen, carbon monoxide, and carbon dioxide increased with rising temperatures and decreased with higher pressures. Conversely, CO conversion and methane selectivity decreased with increased temperature but rose with higher pressure. These outcomes aligned with Le Chatelier's principle for both endothermic and exothermic reactions. The analysis of steam molar flow revealed increased methane conversion due to the higher reaction temperature provided by steam and a higher steam-to-carbon ratio. The simulation demonstrated the economic viability of hydrogen production through the steam methane reforming process. Additionally, it highlighted the significant contribution of steam sales to the overall economic feasibility of the process. Overall, the study underscores the technical feasibility of hydrogen production from natural gas using the steam methane reforming process.

Keywords: *Steam methane reforming, Response surface methodology, CH_4 conversion, Hydrogen selectivity, Process simulation*

1. INTRODUCTION

In recent decades, there has been a growing interest in the utilization of hydrogen, driven by its clean energy characteristics as a fuel and its potential role in addressing the challenges posed by greenhouse gas emissions and global warming [1[. The global shift towards a hydrogen economy is gaining momentum, with hydrogen being envisioned as the future fuel to replace fossil fuels in the quest for a sustainable energy transition and the achievement of net-zero emission goals by 2050 [2].

The extensive use of fossil fuels presents two significant challenges: rapid depletion and environmental pollution. The depletion of fossil fuels raises concerns about energy availability and sustainability, while the environmental impact of fossil fuel usage, particularly the emission of large amounts of carbon dioxide (CO_2), contributes significantly to global warming and climatic issues [3]. Hydrogen emerges as a promising solution to address these challenges, offering a more efficient, and environmentally friendly fuel for sustainable energy development. Additionally, if the source of hydrogen production is fossil-based, it can represent a more efficient utilization of fossil resources [4].

Hydrogen is often considered more as an energy carrier than a direct energy source due to its lighter, cleaner nature, higher energy content,

*Correspondig author: Stanley Toochukwu Ekwueme
E-mail: stanleyekwueme@yahoo.com
Paper received: 11.11.2024.
Paper accepted: 04.01.2025.
The website: https://www.zastita-materijala.org/

and greater efficiency compared to fossil-derived fuels. Commercial hydrogen production encompasses various methods, including production from fossil-based resources like natural gas and coal, as well as renewable means such as water electrolysis [5]. Notably, natural gas-based production, particularly steam reforming, is the most mature and extensively researched large-scale method [6].

Among the technologies for natural gas-based hydrogen production includes steam methane reforming, partial oxidation reforming and autothermal reforming. Partial oxidation reforming or gasification is technically viable but suffers from low efficiency due to a reduced hydrogen yield [7]. In contrast, autothermal reforming combines steam reforming and partial oxidation processes, creating a thermally neutral process that enhances hydrogen production while generating heat. Autothermal reforming is conducted at lower pressures than partial oxidation and is advantageous in that it does not require an external heat source for the reactor, as partial oxidation is exothermic [8, 9]. However, the successful scale-up of autothermal reformers is hindered by two primary challenges: maintaining catalyst stability in the presence of oxygen and effectively controlling temperatures within the reformer. Furthermore, a significant constraint associated with autothermal reforming (ATR) is the substantial investment and operational costs involved in establishing an oxygen production plant dedicated to providing the necessary oxygen for the reaction process[10].

Steam reforming stands out as the most established and widely employed method for hydrogen production using natural gas in industrial applications.The superiority of steam methane reforming over partial oxidation and autothermal reforming lies in its ability to yield more hydrogen product per unit mass of natural gas feedstock [11]. Traditional steam methane reforming technologies have advanced with the integration of carbon capture mechanisms, capturing and utilizing the effluent carbon dioxide (CO_2) gas generated in the process [6].

The process of hydrogen production through SMR involves four distinct steps. These include the pretreatment of the feed gas to eliminate impurities, the reforming of the pre-treated gas to generate synthesis gas, the conversion of carbon monoxide (CO) to hydrogen through a water-gas shift reaction (WGS), and the subsequent recovery and purification to obtain high-purity hydrogen [12].

Research studies have indicated the development and utilization of various catalysts in steam methane reforming (SMR) for hydrogen (H_2) production [2]. Predominantly, these catalysts include supported nickel (Ni) catalysts and a limited number of noble metals such as ruthenium (Ru), rhodium (Rh), palladium (Pd), platinum (Pt), and iridium (Ir). Notably, nickel-based catalysts contribute significantly to SMR research, representing over 60% of total publication outputs [13]. This is attributed to their high activity in H_2 production and cost-effectiveness compared to noble metals. However, a notable drawback of nickel-catalysts is their susceptibility to deactivation through sintering and carbon deposition [14].

To address these challenges, researchers have implemented various strategies, including the use of suitable supports and promoters, as well as optimizing process parameters to mitigate coke formation [14]. Currently, supports like aluminium oxide (Al_2O_3), cerium oxide (CeO_2), lanthanum oxide (La2O3), zirconium oxide (ZrO_2), silicon dioxide (SiO_2), SBA-15, and perovskiteLa FeO_3 have been employed in synthesizing nickel catalysts for SMR. These supports have been observed to exert varying degrees of influence on the stability and activities of nickel catalysts during SMR reactions. Researchers are actively exploring these support materials to enhance the performance and longevity of nickel catalysts in the SMR process[15, 16].

Several researchers have investigated the use of Ni-based catalyst for hydrogen production via SMR. Kim et al. [17] conducted a study where a Ru-doped Ni pellet-type catalyst was prepared for hydrogen production via steam methane reforming. The addition of a small amount of Ru to the Ni catalyst enhanced Ni dispersion, resulting in higher catalytic activity compared to the Ni catalyst alone. During daily startup and shutdown operations, Ni catalysts experienced a significant decrease in CH_4 conversion due to Ni metal oxidation to NiAl2O4, which was not completely reduced at 700 °C. In contrast, the oxidized Ni species in the Ru-Ni catalyst could be reduced under steam methane reforming conditions due to H_2spillover from the Ru surface onto the Ni surface. Consequently, the addition of a small quantity of Ru to the Ni catalyst improved catalytic activity and stability during daily startup and shutdown operations.

Katheria et al. [18] explored the impact of calcination temperature on the stability and activity of Ni/$MgAl_2O_4$ catalysts in SMR. They found that catalyst activity increased with calcination temperature up to 850°C and decreased thereafter due to the formation of nickel aluminate. High pressure was identified as enhancing catalyst stability, and temperature increase correlated with a decrease in the catalyst deactivation rate.

Khanet al. [4] conducted a comprehensive study comparing dry reforming of methane (DRM), steam methane reforming (SMR), and a combination of DRM/SMR using M/ZnLaAlO4 (M = 10%Ni, 3%Pt, 3%Ru) nanocatalysts and 10% Ni/G-Al_2O_3 catalysts. Utilizing the gel combustion technique for supports and wet impregnation for catalysts, they employed FE-SEM and TEM analyses, revealing the nanometric structures of the supports. The findings indicated that 3% Ru/ZnLaAlO4 demonstrated superior catalytic activity in terms of methane conversion and reduced coke formation, showcasing the effectiveness of SMR with this specific catalyst.

Yoo et al. [19] explored the impact of butyric acid in preparing Ni/γ-Al_2O_3 catalysts for SMR. Catalysts were prepared through alumina impregnation with nickel nitrate solution, resulting in mesoporous structures containing a nickel aluminate phase. Nickel dispersion, influenced by the amount of butyric acid used, correlated with methane adsorption capacity. The catalyst prepared with a 0.25 molar ratio of Ni/butyric acid exhibited optimal performance in terms of CH_4 conversion and H_2 yields, demonstrating the significance of preparation conditions on catalyst effectiveness.

Iglesias et al. [20] compared the performance of Ni-based catalysts supported by ceria and ceria doped with 5 wt% of Zr, Pr, or La. Catalysts were obtained through coprecipitation using the urea method, with varying calcination temperatures (600°C, 750°C, and 900°C). Doped catalysts showed enhanced oxygen stability, with Zr-doped catalyst exhibiting the best performance in terms of hydrogen yield and catalyst deactivation. Calcination at 750oC resulted in the highest methane conversion across all cases considered.

Fang et al. [21] investigated the influence of rare earth elements on the physicochemical features of Ni/Ln2Ti2O7 (Ln = La, Pr, Sm, and Y) catalysts for SMR. Employing the co-precipitation and impregnation methods for supports and catalysts, respectively, the study revealed that the transition from La and Pr to Sm and Y supports caused a transformation of the monoclinic layered perovskite to a monoclinic layered pyrochlore structure. Notably, the Ni/Y2Ti2O7 catalyst exhibited superior catalytic activity and resistance to coke formation, showcasing the impact of rare earth elements on catalyst performance.

The complexity of hydrogen production through steam reforming necessitates detailed simulation for optimization. Simulation proves to be a cost-effective alternative to experimentation, offering more efficient process configurations for full deployment[22]. Process optimization ensures the optimal yield of hydrogen products through the judicious allocation of resources and parameters, minimizing costs and heat usage during the process [23]. Several factors influence the performance of the hydrogen production process, including temperature, pressure, steam-carbon ratio, reactor volume, molar flowrate of feedstock, and feed impurities [24]. These parameters impact the reactor differently, and optimizing hydrogen yield involves a meticulous assessment through sensitivity analyses. These analyses evaluate the influence of process parameters (independent variables) on key hydrogen performance outputs, such as methane conversion, hydrogen yield, and hydrogen selectivity. Subsequently, optimization focuses on the parameters with the most significant impact on hydrogen performance [25].

2. STEAM METHANE REFORMING PROCESS

Steam methane reforming is a catalytic process employed for the production of syngas and subsequent extraction of hydrogen through suitable separation methods by utilizing natural gas (methane) and steam. Widely recognized as a commercially mature technology, steam methane reforming has been successfully implemented in various projects [3].

2.1. Chemistry of Steam Methane Reforming

Steam methane reforming involves a series of catalysed reactions occurring in the reactor, primarily the steam methane reforming reaction (1) and the reversed water-gas shift reaction (2):

$$CH_4 + H_2O \leftrightarrow CO + 3H_2 \quad \Delta H = +206kJ/mol \qquad (1)$$

The methane reforming reaction is reversible and can proceed in either direction; however, conditions favour the forward reaction. The water-gas shift reaction (Equation 2) is also integral to the process:

$$CO + H_2O \leftrightarrow H_2 + CO_2 \quad \Delta H = -41KJ/mol \qquad (2)$$

Carbon formation is a potential outcome due to reactions such as carbon monoxide disproportionation (3), methane decomposition (4), and carbon monoxide reduction (5). Ultimately, the SMR process should be configured to limit the occurrence of these reactions. Generally, catalytic steam methane reforming can generate syngas with H_2/CO ratios greater than 5[6]

$$CO \leftrightarrow CO_2 + C \qquad \Delta H = -172.4kJ/mol \qquad (3)$$

$$CH_4 \rightarrow C + 2H_2 \qquad \Delta H = +74.6\,kJ/mol \qquad (4)$$

$$CO + H_2 \leftrightarrow C + H_2O \qquad \Delta H = -131kJ/mol \qquad (5)$$

2.2. Thermodynamics of Steam Methane Reforming Process

Steam methane reforming is an endothermic reaction which favours high temperatures and low pressures. Calculating the Gibbs free energy and equilibrium constants reveals that the reaction requires specific temperatures for optimal activity. An Ellingham-type diagram illustrates the decrease in Gibbs free energy change with an increase in temperature[3].

Methane conversion equilibrium increases with rising temperatures and higher steam-carbon (S/C) ratios but decreases with increasing pressure. Achieving 100% conversion, for example, requires a temperature of 700°C and 1 bar with an S/C of 2.5. At 20 bars, the same conversion necessitates a temperature of 900°C. To reduce coke formation, an S/C of 2.5–3.0 is recommended[6].

Steam methane reforming yields synthesis gas with an H_2/CO ratio of 3:1. The industrial process relies on energy from natural gas combustion, with nickel being the most commonly used catalyst, supported on ceramic oxides or oxide [26].

2.3. Catalysts in Steam Methane Reforming for Hydrogen Production

In the industrial production of hydrogen through steam methane reforming (SMR), catalysts play a pivotal role, with nickel being the preferred choice due to its cost-effectiveness and adequate activity. To further optimize performance, researchers, such as Meloni et al. [26], have proposed shaping the nickel catalyst into multichannel wheels to enhance mass and heat transfer while minimizing pressure drop, particularly in industrial applications. Besides nickel, other catalysts employed in SMR include group VIII metals (iron, cobalt) and precious metals (rhodium, ruthenium, platinum, palladium). However, these alternatives present distinct challenges; iron and cobalt are unstable under partial pressures of steam, and precious metals are economically challenging [27]. Deactivation of Ni-based catalysts due to sintering and coke formation is a known challenge. Ongoing research focuses on addressing these issues by incorporating efficient promoters and support for the base nickel. Commonly used supports for Ni-based catalysts in SMR include α-alumina, magnesia, calcium aluminate, or magnesium aluminate.

Studies reveal that adding small amounts of promoters to the base catalyst significantly suppresses coke formation during SMR. Promoters modify the Ni ensemble size on the surface, inhibiting coke formation. Lanthanides (La, Ce, Gd, Sm) and alkali metals (K) and alkali earth metals (Mg, Ca) have shown promise as promoters for Ni-supported catalysts, enhancing stability [28]. Molybdenum, when added in small amounts, has been found to increase resistance to coking without compromising catalyst activity. Researchers have explored ultra-low concentrations to inhibit coke formation, with unclear mechanisms related to ensemble size control or interference with carbon dissolution during whisker formation.

The choice of support material also influences catalyst performance. Al_2O_3 enhances hydrocarbon cracking and polymerization due to its acidic nature. ZrO2, particularly at low reaction temperatures, outperforms Al_2O_3, attributed to the formation of more hydroxyl groups. MgO promotes surface carbon gasification, hindering coke deposition, while CeO2 prevents coke formation due to its high oxygen storage capacity[6].

Wu et al. [29] presented a comprehensive study on the design, synthesis, and characterization of supported bimetallic Ni-based catalysts for steam reforming. The research focused on modifying Ni with noble metals such as Au and Ag, detailing preparation methods, characterization techniques, and pretreatment approaches. The investigation extended to compare the effects of other metals (Sn, Cu, Co, Mo, Fe, Gd, and B) on catalytic activity, thermal stability, and carbon species in both bimetallic and monometallic Ni-based catalysts. In comparison to monometallic Ni catalysts, Ni-M bimetallic catalysts demonstrated superior performance in methane steam reforming, exhibiting high activity, resistance to carbon formation and sintering of metal particles, and high selectivity for H_2 product. The enhanced catalytic performance of Ni-M bimetallic catalysts was attributed to the synergic effect between the second metal and Ni, leading to the formation of a superficial bimetallic alloy (e.g., Ni-Au, Ni-Ag, Ni-Sn, Ni-Cu, Ni-Co).

Chu et al. [30] improved the catalytic performance of nickel-based catalysts by introducing additives, MgO and FeO, using the impregnation method on micro-channels made of a metal-ceramic complex substrate. Testing these catalysts in the same micro-channel reactor by switching catalyst plates revealed that the Ni-Mg catalyst exhibited the highest activity, especially under harsh conditions, such as high space velocity and/or low reaction temperature. Furthermore, the catalyst's activity and selectivity remained stable during a 12-hour on-stream test, even with a low steam-to-carbon ratio (S/C) of 1.0. The addition of MgO facilitated the dispersion of active Ni species on the substrate, leading to improved catalytic performance in steam methane reforming.

Chanburanasiri et al. [31] conducted a study focusing on a multifunctional catalyst-adsorbent

material for the steam methane reforming process. This material served the dual purpose of catalyzing the reaction and simultaneously adsorbing CO_2. CaO and hydrotalcite (MK30-K) were chosen as supports, replacing the conventional Al_2O_3 support for Ni catalyst. The material, prepared as a powder using the incipient wetness technique, was tested in a fixed bed reactor system. Experimental results revealed that Ni/CaO exhibited lower activity than Ni/Al_2O_3 but achieved high hydrogen concentration in the product stream. The study investigated the effect of Ni loading and found that, under specific conditions (atmospheric pressure, steam-to-methane ratio of 3, and T = 873 K), a loading of 12.5 wt % Ni/CaO was optimal, offering a high hydrogen concentration of 80%. The use of this multifunctional catalyst was shown to eliminate the need for Al_2O_3, thereby requiring a smaller-sized reactor.

2.4. Steps in Steam Methane Reforming Process for Hydrogen Production

The production of hydrogen through steam methane reforming (SMR) involves several key processes, each playing a crucial role in obtaining high-purity hydrogen. The steps include natural gas pre-treatment, the steam methane reforming reaction unit, water-gas shift (WGS) unit, and hydrogen upgrading unit.

2.4.1. Natural Gas Pre-Treatment

Before entering the reformer, natural gas undergoes pre-treatment to remove impurities such as hydrogen sulphide (H_2S) and carbon dioxide (CO_2). Several natural gas treatment processes are available including amine systems, sorption processes etc[6]. However, employing a zinc oxide catalyst, facilitates the removal of acid gases notably H_2S from natural gas according to the equation given below. This is a very economical process and can be used where economy and compactness are critical considerations.

$$NG + H_2S + ZnO \rightarrow ZnS + H_2O + NG \quad (6)$$

This reaction occurs in a guard chamber, reducing the sulphur content to less than 0.1 ppm, a level suitable for the subsequent reforming process.

2.4.2. The Reforming Unit

The reforming unit comprises the pre-reformer, the steam methane reaction unit and the reversed water-gas shift reaction unit. The pre-treated natural gas enters the reformer, starting with pre-reforming to enhance energy efficiency. The pre-reformer converts higher molecular weight hydrocarbons to hydrogen and carbon monoxide. Process steam is introduced, and the mixture is pre-heated before entering the pre-reformer. In the main reformer, methane reacts with process steam to produce synthesis gas (H_2 and CO). The resulting gas is then cooled before entering the WGS unit[6]. The WGS unit enhances hydrogen production by converting carbon monoxide and steam to hydrogen and carbon dioxide in a slightly exothermic reaction. This occurs at 350-500°C, and the gaseous products are cooled before proceeding to the hydrogen separation unit.

The general stoichiometric formula for the pre-reformer reaction is given as

$$C_nH_m + nH_2O \rightarrow \left(n + \frac{m}{2}\right)H_2 + nCO, \text{ For } n \geq 2 \quad (7)$$

Thus, for n=2 to 5, the stoichiometric formula and heat of reaction is given as

$$C_2H_6 + 2H_2O \rightarrow 5H_2 + 2CO\Delta H_{298} = 350\ kJ/mol \quad (8)$$

$$C_3H_8 + 3H_2O \rightarrow 7H_2 + 3CO\Delta H_{298} = 500\ kJ/mol \quad (9)$$

$$C_4H_{10} + 4H_2O \rightarrow 9H_2 + 4CO\Delta H_{298} = 650\ kJ/mol \quad (10)$$

$$C_5H_{12} + 5H_2O \rightarrow 11H_2 + 5CO\Delta H_{298} = 900\ kJ/mol \quad (11)$$

$$C_6H_6 + 6H_2O \rightarrow 13H_2 + 6CO\Delta H_{298} = 1050\ kJ/mol \quad (12)$$

CO methanation reaction also occurs in the system to produce methane from the reaction of CO and H_2 according to the equation below

$$CO + 3H_2 \rightarrow CH_4 + H_2O \quad \Delta H_{298} = 650\ kJ/mol \quad (13)$$

2.4.3. Hydrogen Upgrading Unit

The product gaseous stream, comprising hydrogen, carbon monoxide, steam, carbon dioxide, and unconverted methane from the reactor, undergoes separation using pressure swing adsorption (PSA) or amine systems. This process occurs at high pressure and low temperature, resulting in high-purity hydrogen (up to 99.95%). Some steam produced is utilized in the process, while the remaining can be used or sold. Additionally, these plants often integrate carbon dioxide capture technology to mitigate environmental impacts.

3. METHODS

The methods include the simulation of hydrogen production from SMR. First, the kinetic model is presented with relevant kinetic parameters required by the simulator. Next the simulation is performed and optimisation are performed based on process configuration and sensitivity analyses on reaction conditions and input factors.

3.1. Kinetic Model of Steam Methane Reforming

The kinetic models are mathematical models developed from experimental studies performed

using specific catalysts at specified operating conditions and are unique for a specified reaction process. The kinetic model utilized in this study for hydrogen production from steam reforming of methane are based on the works of Abbas et al [6] over 18 wt. % NiO/a-Al_2O_3.

The kinetic model for reaction 1 (for equation1) represented as (R1) is given in equation 14 while the reaction 2 (for equation 2) represented as (R2) is given in equation 15

$$R_1 = \frac{k_1}{P_{H_2}^{2.5}}\left(P_{CH_4}P_{H_2O} - \frac{P_{H_2}^3 P_{CO}}{K_{eq1}}\right)\left(\frac{1}{\Omega^2}\right) \quad (14)$$

$$R_2 = \frac{k_2}{P_{H_2}}\left(P_{CO}P_{H_2O} - \frac{P_{H_2}P_{CO_2}}{K_{eq2}}\right)\left(\frac{1}{\Omega^2}\right) \quad (15)$$

$$\Omega = 1 + K_{CO}P_{CO} + K_{H_2}P_{H_2} + K_{CH_4}P_{CH_4} + K_{H_2O}\frac{P_{H_2O}}{P_{H_2}} \quad (16)$$

The equilibrium constants $K_{eq1}$and K_{eq2} are given below

$$K_{eq1} = exp\left(\frac{-28630}{T} + 30.114\right) \quad (17)$$

$$K_{eq2} = exp\left(\frac{4400}{T} - 4.036\right) \quad (18)$$

The kinetic constant (rate constant) is expressed as a function of a preexponential factor and an activation energy following the Arrhenius expression given below in (19)

$$k_i = k_{i,0}exp\left(-\frac{E_{A,i}}{RT}\right) \quad (19)$$

The adsorption equilibrium constant is expressed as a function of the pre-exponential factor and the adsorption enthalpies following the Vant Hoff's expression as given in (20)

$$K_j = K_{j,0}exp\left(-\frac{\Delta H_j}{RT}\right) \text{for j= A, B, and P} \quad (20)$$

$k_i$is the rate constant, mmolg^{-1}min^{-}bar$^{-2.5}$

$k_{i,0}$is the pre-exponential factor for the rate constant, mmolg^{-1}min^{-}bar$^{-2.5}$

$K_j$is the adsorption equilibrium constant, mmolg^{-1}min^{-}bar$^{-2.5}$

$K_{j,0}$is the pre-exponential factor for the adsorption equilibrium constant, mmolg^{-1}min^{-}bar$^{-2.5}$

$\Delta H_j$is the adsorption enthalpy change, kJ/mol

T is the temperature in kelvin

Ea is the activation energy, kJ/mol

R is the universal molar gas constant, 8.314 J/mol-K

The kinetic parameters corresponding to the kinetic model for R1 and R2 is given in Table 1

Table 1. Kinetic parameters used for the simulation [6]

Parameter	Value	Unit
k_1	1.17E12	molbar$^{-0.5}$g^{-1}s^{-1}
k_2	5.42E2	molbar$^{-0.5}$g^{-1}s^{-1}
E_1	240.10	kJ/mol
E_1	67.12	kJ/mol
KH_2	6.12E-09	bar$^{-0.1}$
ΔHH_2	-82.9	kJ/mol
KCO	8.23E-05	bar$^{-0.1}$
ΔHCO	-70.61	kJ/mol
KH_2O	1.77E-05	bar$^{-0.1}$
ΔHH_2O	88.6	kJ/mol
$K\mathrm{CH}_4$	6.65E-04	bar-0.1
$\Delta H\mathrm{CH}_4$	-38.28	kJ/mol

3.2. Reactor Performance Calculation

There are three important parameters that are used to assess the performance of the reactor during simulation. These includes the conversion, the selectivity and the yield. The definitions of these parameters are given as

$$Conversion = \frac{(Reactants\ consumed\ in\ the\ reactor)}{(Reactants\ fed\ to\ the\ reactor)}\ x\ 100 \quad (21)$$

$$Selectivity = \\ = \frac{(Desired\ product\ produced\ in\ the\ reactor)}{(Reactants\ consumed\ in\ the\ reactor)}\ x\ 100 \quad (22)$$

$$Yield = \frac{(Desired\ product\ produced\ in\ the\ reactor)}{(Reactants\ fed\ to\ the\ reactor)}\ x\ 100 \quad (23)$$

It is important to calculate the methane conversion and selectivity, the hydrogen yield and selectivity, the CO_2 and CO selectivities which are all given in the equations below

$$CH_4\ Conversion: X_{CH_4}(\%) = \frac{V_{CH_4,in} - V_{CH_4,out}}{V_{CH_4,in}}\ x\ 100 \quad (24)$$

The formula for hydrogen yield (% wtCH_4) is given as

$$H_2\ Yield\ (\%)\ (\%\ wt\ CH_4) = \frac{(V_{H_2,out}\ x\ MW\ of\ H_2)}{(V_{CH_4,in}\ x\ MW\ of\ CH_4)}\ x\ 100 \quad (25)$$

The selectivity of hydrogen is given as

$$H_2\ Selectivity: S_{CH_4}(\%) = \frac{V_{H_2,out}}{(V_{CH_4,out} + V_{H_2,out})}\ x\ 100 \quad (26)$$

The selectivity of methane is given as

$$CH_4\ Selectivity: S_{CH_4}(\%) = \frac{V_{CH_4,out}}{(V_{CH_4,out} + V_{CO_2,out} + V_{CO,out})} x\ 100 \quad (27)$$

The selectivity of carbon dioxide is given as

$$CO_2\ Selectivity: S_{CO_2}(\%) = \frac{V_{CO_2,out}}{(V_{CH_4,out} + V_{CO_2,out} + V_{CO,out})} x\ 100 \quad (28)$$

The selectivity of carbon monoxide is given as

$$CO\ Selectivity: S_{CO}(\%) = \frac{V_{CO,out}}{(V_{CH_4,out} + V_{CO_2,out} + V_{CO,out})} x\ 100 \quad (29)$$

Where $V_{H_2,out}, V_{CH_4,out}, V_{CO_2,out}, V_{CO,out}$ are the outlet molar flowrate of hydrogen, methane, CO_2, and CO respectively and $V_{CH_4,}$ is the inlet molar flowrate of methane.

3.3. Model Simulation

The comprehensive process simulation model for hydrogen production via steam methane reforming, consists of three interconnected units arranged in series which are the pre-reformer unit, the reforming units, and the hydrogen upgrading unit. All simulations were executed using Aspen Hysysv11 software, employing the Peng Robinson fluid property package. The simulation process is summarized using the block diagram in figure 1

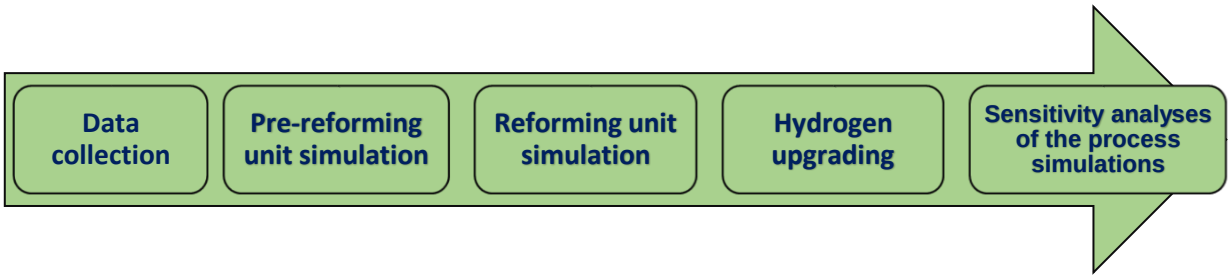

Figure 1. Block diagram of simulation procedures

As seen in Figure 1, the initial step involves the collection of data, ensuring its accuracy through validation to confirm its representativeness of the process system. Subsequently, the simulation progresses to the pre-reformer unit, where higher molecular mass hydrocarbons in the natural gas feedstock undergo conversion to methane. Moving to the reforming unit, distinct reactors are employed to model steam methane reactions and water-gas shift (WGS) reactions, strategically arranged in series. It is within the reforming unit that the actual hydrogen production occurs. To enhance the purity of hydrogen, the hydrogen upgrading unit is implemented. In this study, the upgrading unit is simulated as an adsorption process system using the Hysys splitter. The splitter functions to divide the outlet stream from the reforming unit into two streams: one containing hydrogen gas and the other containing undesired reactor product impurities.

3.3.1. Data Gathering

The input dataset includes information on the composition of natural gas, reactor and catalyst specifications, and the initial conditions of the reactor feed. The natural gas utilized was sourced from the Assa field in Ohaji North, Imo State, situated in the Niger Delta region of Nigeria. This natural gas underwent field processing to eliminate impurities. Sampling at the separator was conducted using the surface sampling method, and the collected natural gas sample was subjected to characterization to determine its molar composition. The composition of the natural gas used is given in Table 2

Table 2. Composition of natural gas feedstock (Assa field)

Component	Mole fraction
Methane	0.966934
Ethane	0.015310
Propane	0.003229
i-Butane	0.001763
n-Butane	0.001950
i-Pentane	0.000941
n-Pentane	0.000700
n-Hexane	0.000259
n-Heptane	0.000224
n-Octane	0.000160
n-Nonane	0.000161
Nitrogen	0.000101
CO_2	0.008269

Table 2 shows the mole fraction composition of individual components in the natural gas feedstock. The composition reveals that the natural gas is a rich gas primarily composed of methane, along with lesser quantities of higher molecular mass hydrocarbons and non-hydrocarbon impurities. The conditions of the reactor feeds at inlet are given in Table 3 while the reactor and catalyst data are given in Table 4 below

Table 3. Inlet conditions of the Feed stream [6]

Parameter	Value	
	Natural gas	**Steam**
Molar flow	1992 kmol/hr (40 MMscfd)	4981 kmol/hr (100 MMscfd)
Inlet temperature	40oC	252oC
Inlet pressure	30 bars	30 bars

Table 4. Reactor and catalyst data [6]

Parameter	Value
Tube length	12 m
Number of tubes	67500
Tube diameter	0.025 m
Wall thickness	0.005 m
Total tube Volume	400 m^3
Void fraction	0.45
Catalyst solid density	1010 kg/m^3
Catalyst particle diameter	0.01 m

3.3.2. Pre-Reformer Simulation

To prevent the formation of soot, a pre-reformer was introduced upstream of the main reformer unit, aiming to convert higher molecular mass hydrocarbons (non-methane hydrocarbons) from the natural gas feed. The pre-reformer operation is crucial to enhance the reformer's operability and catalyst activity by avoiding deactivation due to sintering, ultimately improving the efficiency of the reaction process. The pre-reformer was simulated as a conversion reactor in Aspen Hysys.

Before entering the pre-reformer, 40 MMscfd of natural gas at a temperature and pressure of 40°C and 30 bar, respectively, were preheated to 252°C using a heater. Simultaneously, 50 MMscfd of water at 252°C and 30 bar was introduced into the pre-reformer. Reactions within the pre-reformer converted the natural gas into methane gas. The pre-reformer outlet comprised a stream with a molar flowrate of 7047 kgmol/h, a temperature of 191.1°C, and a pressure of 30 bars.

3.3.3. Steam Methane Reforming Simulation: Base Case

Following the pre-reformer unit, the base case simulation was conducted in the steam methane reforming unit to assess system performance and identify potential optimization parameters. The reforming simulation included the steam methane reaction and the water-gas shift (WGS) reaction. Three reactors were modelled in the reforming unit: the first for the steam methane reaction and the subsequent two, placed in series, for the high-temperature and low-temperature WGS reactions. All three reactors were modelled as plug flow reactors in Aspen Hysys, effectively representing a multi-tubular fixed-bed catalytic reactor that aptly describes the multiple reaction sets considered in this study.

Due to the endothermic nature of the steam methane reaction, a high temperature was necessary. The outlet stream from the pre-reformer, with a temperature of 275.2°C, was heated to 1000°C for the steam methane reaction. It is crucial to note that, while the highly endothermic nature of the steam methane reaction requires high temperatures for thermodynamic processing, a temperature limit of 1028°C was set as the maximum operational temperature to prevent soot formation in the reactor during the steam methane reforming (SMR) process. The inlet to the steam methane reaction reactor comprised methane and steam with small amounts of CO and CO_2. The methane underwent conversion in the steam methane reactor, producing hydrogen gas alongside CO through the reaction of methane and steam. To enhance hydrogen production, the outlet stream from this reactor was directed to the WGS reactor, aimed at increasing hydrogen yield by converting CO products from the upstream reactor.

The first WGS reactor was the high-temperature WGS reactor, with an inlet stream temperature and pressure of 490.1°C and 30 bars, respectively. Downstream of the high-temperature WGS reactor, the fluid was sent to the low temperature shift reactor (LTSR). The WGS reactors facilitated CO shift, increasing hydrogen yield while producing CO_2. The outlet stream of the LTWGS reactor was then cooled to 30°C before entering the upgrading unit, modelled as a splitter. The splitter simulated the separation of hydrogen gas from undesired reaction products.

The process flow diagram (PFD) for the integrated process model is depicted in Figure 2.

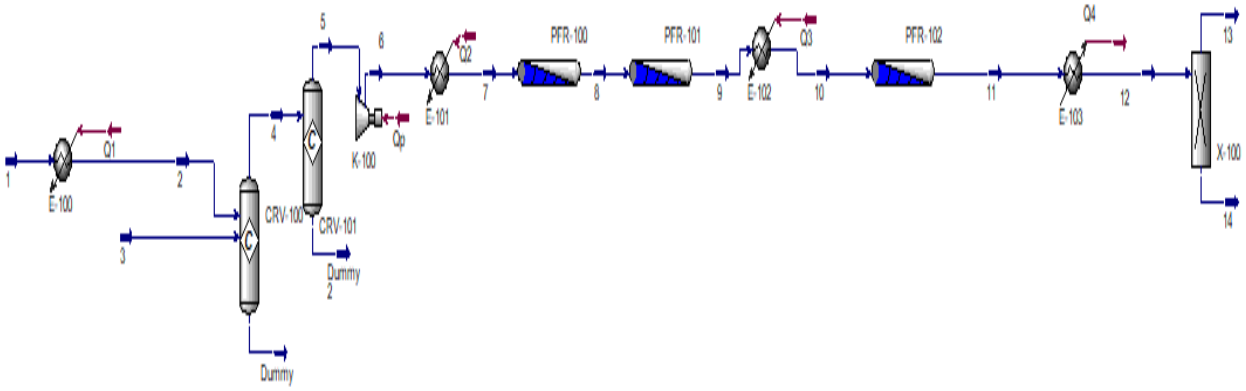

Figure 2. Hysys Process flow diagram (PFD) for base case simulation

3.3.4. Sensitivity Analyses of the Process

Sensitivity analyses were conducted to evaluate the impact of varying process conditions on reactor performance. These analyses provide insights into potential optimization opportunities by identifying key process parameters that positively influence reactor performance. Utilizing these parameters, optimization strategies and schedules for the process system can be developed, with the overarching goal of enhancing hydrogen yield while minimizing energy consumption and overall costs in the system. The sensitivity analyses conducted in this study focused on investigating the effects of the following parameters on reactor conversion, selectivity, and yield: Reactor Inlet Temperature, Reactor Inlet Pressure, Reactor Volume, Molar Flow Rate of Steam, Steam-Carbon Ratio. By systematically studying these parameters, the sensitivity analyses provide valuable information for developing effective strategies to optimize the plant's performance and achieve higher hydrogen yields, while minimizing energy consumption and operational costs.

4. RESULTS

Results of the simulations performed are presented and discussed. Sensitivity analyses results are mostly highlighted to show the impact of the input factors on the performance of the system and how it affects the optimisation of the SMR plant.

4.1. Effect of Temperature

In the steam methane reforming process, temperature is a critical factor influencing both the endothermic steam methane reforming reaction and the slightly exothermic water-gas shift reaction. Figure 3 illustrates the impact of temperature on the conversion of methane and carbon monoxide in the steam methane reforming and water-gas shift reactors, respectively.

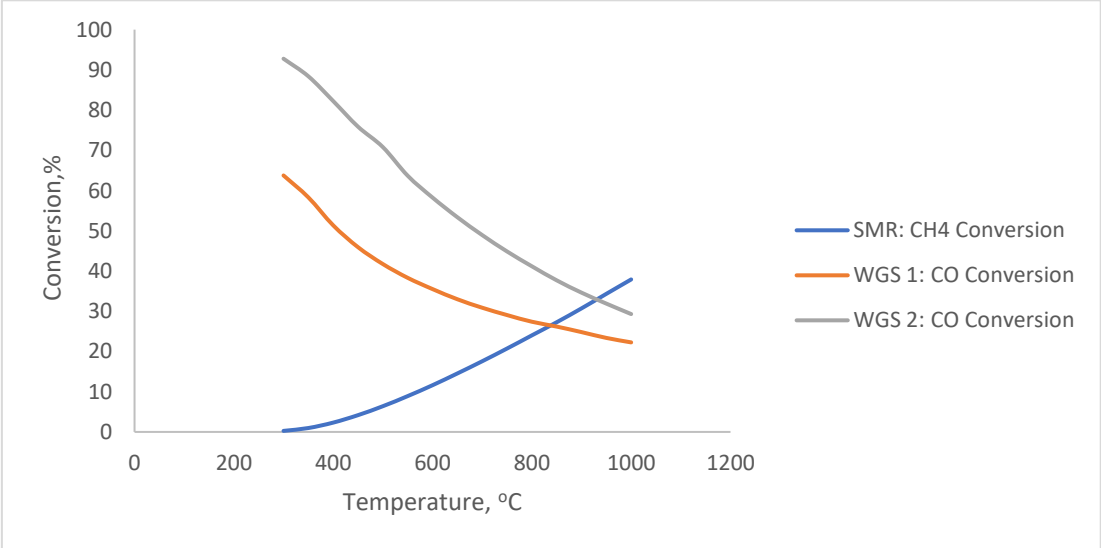

Figure 3. Effect of temperature on conversion in the reformer unit for P=40 bar and S/C=2.24

Figure 3 clearly indicates that the methane conversion in the steam methane reactor increases with an increase in temperature. This aligns with expectations for an endothermic reaction, as higher temperatures favour the thermodynamic feasibility of the methane conversion reaction. increasing the temperature from 600°C to 800°C resulted in an increase in methane conversion from 11.61% to 23.99%. Endothermic reactions demand significant heat input for thermodynamic progression, and higher temperatures facilitate this input, promoting the forward reaction of methane conversion into synthesis gas, comprising hydrogen and carbon monoxide.

Conversely, higher temperatures led to a decrease in carbon monoxide (CO) conversion in the two water-gas-shift reactions. Lower temperatures are more advantageous for achieving higher carbon monoxide (CO) conversions in the water gas-shift reactor. This behaviour is attributed to the exothermic nature of the water gas-shift reactions, which approach equilibrium at lower temperatures due to thermodynamic constraints. Special catalysts are employed to alleviate kinetic limitations at high temperatures since reaction rates tend to be higher at elevated temperatures. Increasing the temperature from 600°C to 800°C reduced carbon monoxide (CO) conversion from 35.51% to 27.39% and from 58.25% to 41.18% for the first water gas-shift and the second water gas-shift reactors, respectively.

The impact of temperature on the selectivity of hydrogen, methane, carbon monoxide, and carbon dioxide is evident in Figure 4.

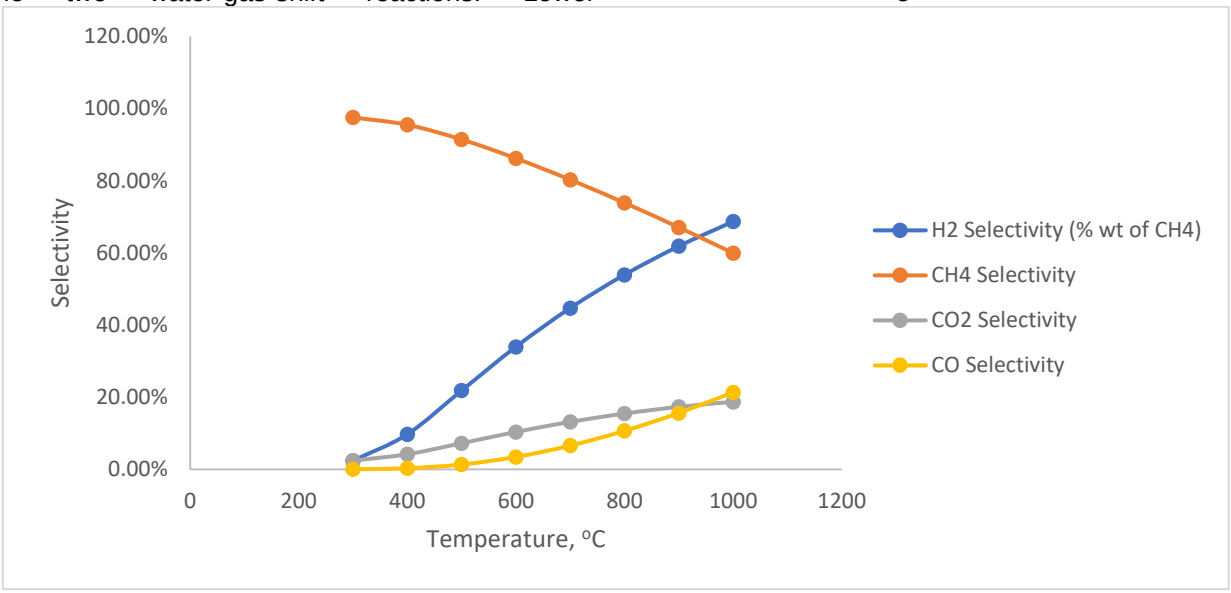

Figure 4. Effect of temperature on Selectivity of gaseous products for P=40 bar and steam to carbon (S/C=2.24)

Figure 4 explored the selectivities of hydrogen, methane, carbon monoxide, and carbon dioxide by varying the temperature. The results revealed that with increasing temperature, the selectivity of methane decreased, while the selectivities of hydrogen, carbon monoxide, and carbon dioxide increased. This phenomenon is attributed to the higher conversion of methane at elevated temperatures, resulting in larger amounts of hydrogen, carbon monoxide, and carbon dioxide and consequently increasing their selectivities. For example, a higher selectivity of methane, reaching up to 97.53%, was observed at a pressure and temperature of 40 bar and 300°C, respectively. Furthermore, the selectivity of hydrogen benefited from higher temperatures, with a selectivity of 68.68% recorded at a pressure and temperature of 40 bar and 1000°C.

The hydrogen yield, expressed as a percentage of the weight of methane, was also scrutinized and presented in Figure 5.

Figure 5 demonstrates the impact of temperature on the hydrogen yield throughout the entire SMR process. The trend indicates that higher temperatures lead to increased hydrogen yield. However, even at a pressure of 40 bar and a high temperature of 1000°C, the hydrogen yield remains relatively modest, recording only 16.8%.

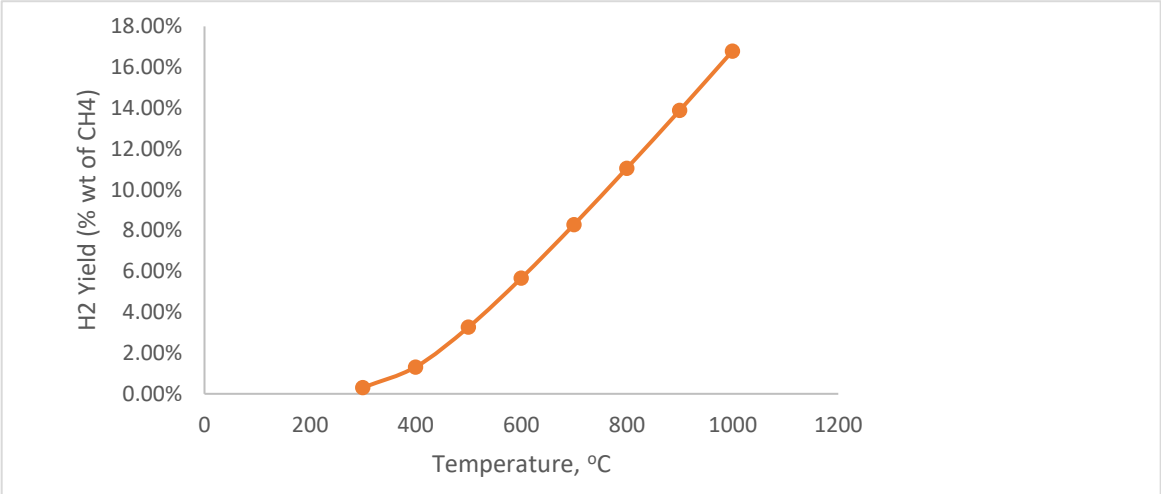

Figure 5. Effect of temperature on the hydrogen yield (% wt of Methane) for P=40 bar and (S/C=2.24)

4.2. Effect of Pressure

Pressure significantly influences the design and operation of the SMR process. The selection of appropriate pressures is critical due to the nature of the two reactions involved: the endothermic Steam Methane Reforming reaction and the exothermic Water-Gas Shift (WGS) reaction. Le Chatelier's principle suggests that lower pressures are more favourable for endothermic reactions, while higher pressures are more favourable for exothermic reactions. The effects of pressures at a temperature of 1000°C and a Steam-to-Carbon (S/C) ratio of 2.24 have been investigated, as depicted in Figure 6, Figure 7 and Figure 8.

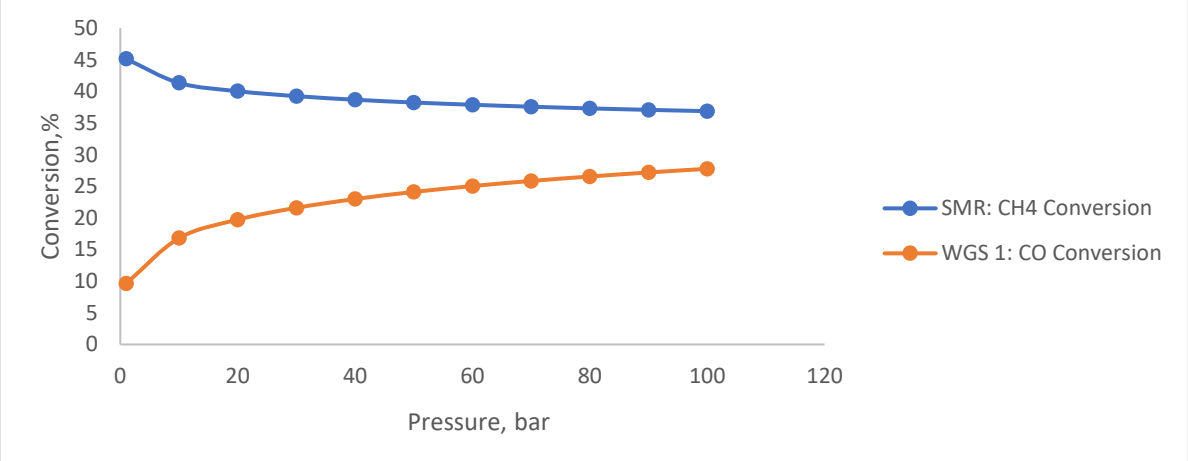

Figure 6. Effect of pressure on the methane and carbon monoxide conversions at a temperature of 1000ºC and steam to carbon (S\C=2.24).

Figure 6 demonstrates the impact of pressure on methane and carbon monoxide conversions in the steam methane reforming and water-gas shift reactors. The plot indicates that as pressure increases, methane conversion in the steam methane reforming reactor decreases, while carbon monoxide conversion in the water-gas shift reactor increases. These trends align with Le Chatelier's principle for endothermic and exothermic reactions, respectively. Notably, the influence of pressure on component conversion is more pronounced at lower pressures compared to higher pressures. To illustrate this, let's compare conversions between 1 bar and 10 bars with those between 90 bar and 100 bar.

In the steam methane reforming reaction, methane conversion decreases from 45.14% to 41.35% as pressure increases from 1 bar to 10 bars, resulting in an 8.4% decrease. However, when pressure rises from 90 bars to 100 bars, methane conversion only decreases from 37.09% to 36.88%, representing a mere 0.57% decrease. Thus, changes in pressure have a greater impact on methane conversion at lower pressure ranges than at higher pressure ranges in the steam methane reforming reactor.

Similarly, in the water-gas shift reaction, carbon monoxide conversion increases from 9.64% to 16.8% as pressure rises from 1 bar to 10 bars, indicating a substantial 74.31% increase. However, when pressure increases from 90 bars to 100 bars, carbon monoxide conversion only increases from 27.19% to 27.77%, representing a modest 2.13% increase. Consequently, changes in pressure have a more significant effect on carbon monoxide conversion at lower pressure ranges than at higher pressure ranges in the water-gas shift reactor.

The effect of pressure on the selectivities of hydrogen, methane, carbon monoxide, and carbon dioxide is shown in Figure 7.

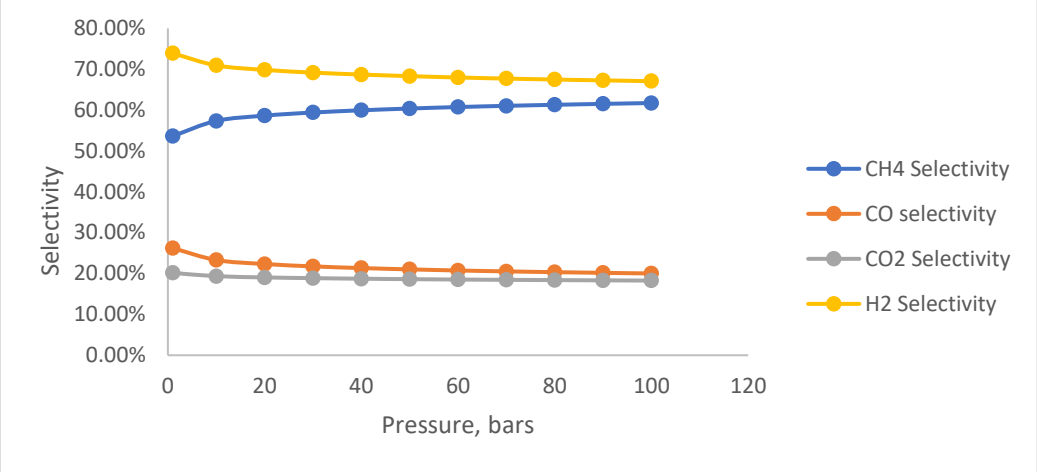

Figure 7. Effect of pressure on product selectivity of gases at a temperature of 1000°C and steam to carbon ratio (S/C=2.24).

Figure 7 illustrates the selectivity of different components relative to pressure. Hydrogen demonstrates the highest selectivity, followed by methane and carbon monoxide, while carbon dioxide exhibits the least selectivity under varying pressures. Increasing pressure results in decreased selectivity for hydrogen, carbon monoxide, and carbon dioxide, whereas methane selectivity increases with rising pressure. Importantly, the influence of pressure on selectivity is more pronounced at lower-pressure ranges compared to higher-pressure ranges.

Figure 8 specifically examines the impact of pressure on hydrogen yield.

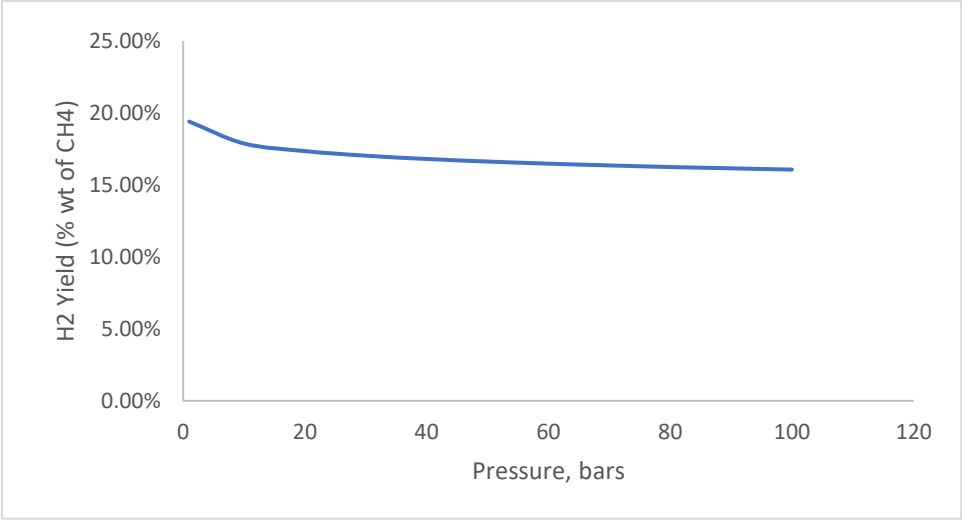

Figure 8. Effect of pressure hydrogen yield at a temperature of 1000°C and steam to carbon ratio (S/C=2.24)

Figure 8 depicts the relationship between pressure and hydrogen yield. The graph indicates that the hydrogen yield decreases with an increase in pressure. A substantial decrease in hydrogen yield is evident between 1 bar and 10 bars, but the curve starts to level off as pressure continues to

rise from 20 bars to 100 bars. Hence, the hydrogen yield is more responsive to changes in lower-pressure ranges compared to higher-pressure ranges.

4.3. Effect of Reactor Volume

The reactor volume is a pivotal factor influencing the conversion of reactants to products by offering the required space for the reaction. Insufficient reactor volume can lead to inadequate space during the reaction time, hindering the reaction from reaching equilibrium. Figure 9 outlines the effects of varying reactor volumes on methane and carbon monoxide conversions.

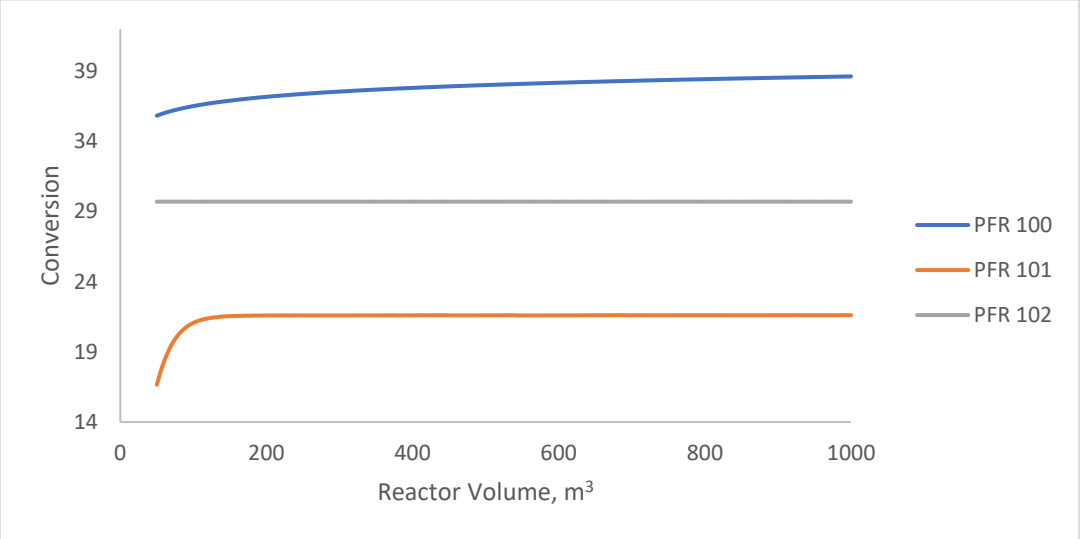

Figure 9. Effect of reactor volume on component conversion in the PFR reactors

Figure 9 illustrates the effect of reactor volume on methane conversion in the SMR reactor and carbon monoxide conversion in the steam-to-carbon ratio reactors. Upon examination of the plot, it is evident that reactor volume has a relatively minor impact on methane conversion. An increase in reactor volume from 397.6 m^3 (base case) to 1000 m^3 resulted in a modest improvement in methane conversion, rising from 37.8% to 38.62%, representing a 2.17% increase. Concerning the first steam-to-carbon ratio reactor, carbon monoxide conversion increased with the expansion of reactor volume up to 150 m^3. However, for the second steam-to-carbon ratio reactor, reactor volume had no discernible effect on carbon monoxide conversion, remaining constant irrespective of changes in reactor volume. Beyond this point, further increases in reactor volume led to negligible changes in carbon monoxide conversion. Overall, reactor volume demonstrated a relatively modest impact on component conversions.

4.4. Effect of Molar Flow of Steam

Figure 10 investigated the effect of the molar flow of steam while maintaining a constant molar flow of carbon, thereby altering the steam-to-carbon ratio (S/C ratio).

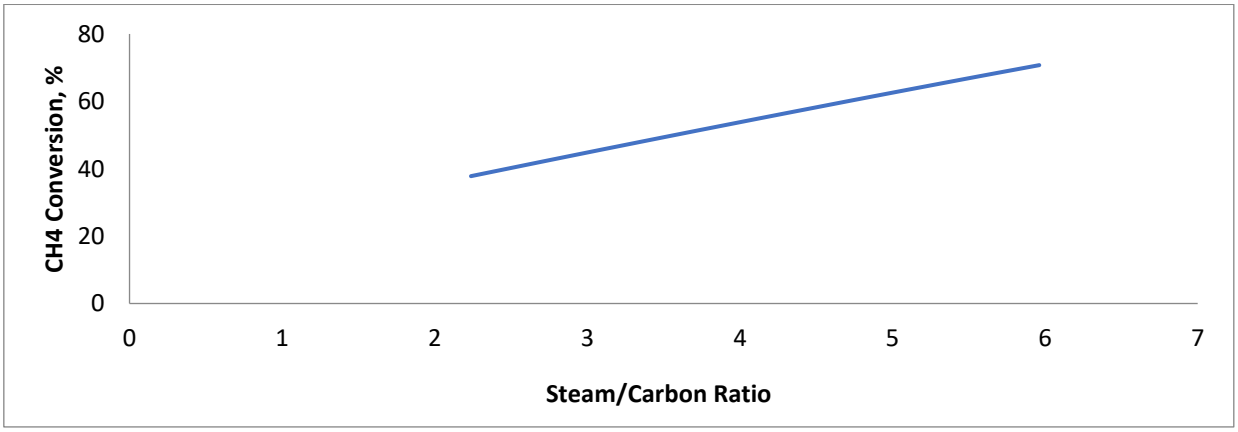

Figure 10. Effect of S/C ratio on Methane conversion for a temperature of 1000°C and pressure of 40 bars

This ratio signifies the amount of steam available per molar flow of carbon and significantly influences the conversion of methane to synthesis gas. Inadequate steam supply may lead to incomplete methane conversion and the formation of soot in the reactor. To ensure optimal methane conversion and prevent soot formation, careful regulation of the steam flow is essential. In this study, the molar flow of methane to the SMR reactor remained constant at 2034.7 kgmol/h, while the molar flowrate of steam varied between 4552.8 kgmol/h and 12130.93 kgmol/h. This variation resulted in different steam-to-carbon ratios of 2.24, 3.47, 4.72, and 5.96, corresponding to steam molar flows of 4552.8 kgmol/h, 70068.98 kgmol/h, 9597.53 kgmol/h, and 12130.93 kgmol/h, respectively.

In Figure 10, the influence of the steam carbon ratio on methane conversion is depicted at a temperature of 1000°C and a pressure of 40 bars. The graph illustrates that methane conversion increases with an elevated steam-to-carbon ratio. This correlation is anticipated because a higher steam-to-carbon ratio supplies more steam for the reaction, facilitating the conversion of carbon to the desired products. However, it is essential to consider that an increased steam-to-carbon ratio results in higher energy requirements, as more steam production becomes necessary. Consequently, this factor impacts the overall operational cost of the process. Therefore, determining an optimal steam-to-carbon ratio involves conducting cost-benefit analyses considering the desirable products obtained from the molar flow of steam.

Moreover, the rationale behind the rise in methane conversion due to an elevated S/C ratio lies in the greater temperature variation along the reactor's length. This temperature variation provides higher heat for the endothermic steam methane reforming (SMR) reaction. Figure 11 visually represents this phenomenon.

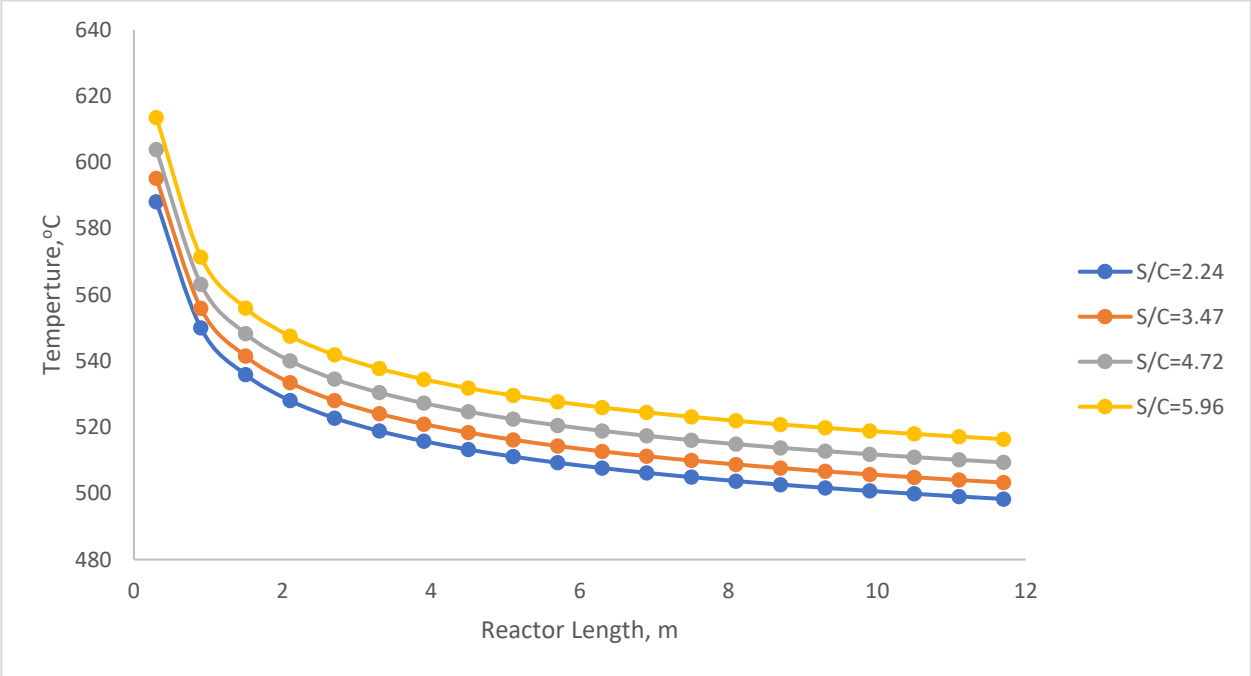

Figure 11. Temperature variation with length in the SMR reactor due to changes in steam to carbon (S/C ratio at P=40 bar and 1000°C temperature)

Figure 11 illustrates the temperature profile within the steam methane reactor, spanning from the reactor inlet to the reactor outlet. A higher steam-to-carbon ratio correlates with increased reaction temperatures along the reactor. This can be attributed to the augmented molar flow of steam, which enhances heat transfer to the reaction component stream within the reactor. Consequently, the temperature of the reaction phases increases. Additionally, the outlet temperature of the reactor increases with an increased steam-to-carbon ratio.

The increased reaction temperatures attained in the SMR reactor play a crucial role in the endothermic nature of the process. Higher temperatures contribute to greater methane conversion, as observed in Figure 10. This phenomenon can be attributed to the increased availability of heat within the reactor, promoting the conversion of methane to desired products.

5. CONCLUSION

This study utilized Aspen HysysV11 software with the Peng Robinson property package to conduct a comprehensive simulation of hydrogen gas production through steam reforming of methane. The investigation focused on employing Abbas et al [6] over 18 wt. % NiO/a-Al_2O_3catalyst. The simulations explored the influence of various process parameters methane conversion, hydrogen selectivity and yield, methane selectivity, carbon monoxide selectivity and yield, carbon dioxide selectivity and yield, hydrogen to carbon monoxide ratio, and hydrogen production.

The results revealed that higher temperatures positively impacted methane conversion, hydrogen selectivity, and yield, aligning with Le Chatelier's principle for endothermic reactions. However, the carbon monoxide conversion in the water gas shift (WGS) reactor decreased with increasing temperature, indicative of an exothermic reaction process. Additionally, selectivities for hydrogen, carbon monoxide, and carbon dioxide increased with temperature due to higher methane conversions, resulting in elevated volumes of hydrogen, carbon monoxide, and carbon dioxide. Conversely, methane selectivity decreased with temperature. Sensitivity analysis on hydrogen yield demonstrated an increase with temperature.

Furthermore, the study indicated a decrease in methane conversion with higher pressure, while carbon monoxide conversion in the WGS reactor increased, consistent with Le Chatelier's principle. Selectivities for hydrogen, carbon monoxide, and carbon dioxide decreased with increasing pressure, while methane selectivity increased. Hydrogen exhibited the highest selectivity, followed by methane and carbon monoxide, with carbon dioxide showing the least selectivity under pressure. This was attributed to the WGS shift reactor which favoured hydrogen production over carbon monoxide. Hydrogen yield decreased with higher pressure.The examination of steam molar flow revealed that methane conversion increased with a higher steam molar flow due to the elevated reaction temperature provided by steam and a higher steam-to-carbon ratio.

6. REFERENCES

[1] J.Gorrea, F. Ortloff, C. van Leeuwenc (2019) Production costs for synthetic methane in 2030 and 2050 of an optimized Power-to-Gas plant with intermediate hydrogen storage. Applied Energy 253: 113594

[2] A.O.Oni, K.Anaya, T. Giwa, G. Di Lullo, A. Kumar (2022) Comparative assessment of blue hydrogen from steam methane reforming, autothermal reforming, and natural gas decomposition technologies for natural gas-producing regions. Energy Conversion and Management 254: 115245, https://doi.org/10.1016/j.enconman.2022.115245

[3] K. Liu, C. Song, & V. Subramani. (2010). Hydrogen and syngas production and purification technologies. John Wiley & Sons.

[4] M. H. A. Khan, R. Daiyan, P. Neal, N. Haque, I. MacGill, & R. Amal. (2021). A framework for assessing economics of blue hydrogen production from steam methane reforming using carbon capture storage & utilisation. International Journal of Hydrogen Energy, 46(44), 22685–22706.

[5] T. N. Do, H. Kwon, M. Park, C. Kim, Y. T. Kim, & J. Kim. (2023). Carbon-neutral hydrogen production from natural gas via electrified steam reforming: Techno-economic-environmental perspective. Energy Conversion and Management, 279, 116758.

[6] S. Z. Abbas, V. Dupont, & T. Mahmud. (2017). Kinetics study and modelling of steam methane reforming process over a NiO/Al_2O_3 catalyst in an adiabatic packed bed reactor. International Journal of Hydrogen Energy, 42(5), 2889–2903.

[7] S. Dermühl& U. Riedel. (2023). A comparison of the most promising low-carbon hydrogen production technologies. Fuel, 340, 127478.

[8] C. Joo, J. Lee, Y. Kim, H. Cho, B. Gu, & J. Kim. (2023). A novel on-site SMR process integrated with a hollow fiber membrane module for efficient blue hydrogen production: Modeling, validation, and techno-economic analysis. Applied Energy, 354, 122227.

[9] N. Chalkiadakis, E. Stamatakis, M. Varvayanni, A. Stubos, G. Tzamalis, & T. Tsoutsos. (2023). A new path towards sustainable energy transition: Techno-economic feasibility of a complete hybrid small modular reactor/hydrogen (SMR/H_2) energy system. Energies, 16(17), 6257.

[10] H. Song, Y. Liu, H. Bian, M. Shen, & X. Lin. (2022). Energy, environment, and economic analyses on a novel hydrogen production method by electrified steam methane reforming with renewable energy accommodation. Energy Conversion and Management, 258, 115513.

[11] Z. Navas-Anguita, D. García-Gusano, J. Dufour, & D. Iribarren. (2021). Revisiting the role of steam methane reforming with CO_2 capture and storage for long-term hydrogen production. Science of the Total Environment, 771, 145432.

[12] S. Rajyalakshmi, K. Patwardhan, & P. V. Balaramakrishna. (2012). Modelling optimisation of process and design parameters for minimising natural gas consumption in hydrogen production by steam reforming. PTQ Q1, 1–6.

[13] K. S. Ullah, A. Omer, K. Rashid, N. U. Rehman, I. Rahimipetroudi, S. D. Kim, & S. K. Dong. (2023). Modelling and comprehensive analysis of hydrogen production in a newly designed steam methane

reformer with membrane system. Computers & Chemical Engineering, 175, 108278.

[14] B. V. Ayodele, S. I. Mustapa, M. Y. B. MohdYassin, & S. Abdullah. (2019). Experimental and optimization studies of hydrogen production by steam methane reforming over lanthanum strontium cobalt ferrite supported Ni catalyst. International Journal of Energy Research, 43(14), 8118–8135.

[15] A. Amini, M. H. Sedaghat, S. Jamshidi, A. Shariati, & M. R. Rahimpour. (2023). A comprehensive CFD simulation of an industrial-scale side-fired steam methane reformer to enhance hydrogen production. Chemical Engineering and Processing - Process Intensification, 184, 109269.

[16] A. A. D. Zare, M. Yari, H. Nami, & F. Mohammadkhani. (2023). Low-carbon hydrogen, power and heat production based on steam methane reforming and chemical looping combustion. Energy Conversion and Management, 279, 116752.

[17] T. Y. Kim, J. H. Lee, S. Jo, J. Kim, J. H. Woo, R. Dhanusuraman, ...& S. C. Lee. (2023). Improving the stability of Ru-doped Ni-based catalysts for steam methane reforming during daily startup and shutdown operation. Catalysts, 13(6), 949.

[18] S. Katheria, A. Gupta, G. Deo, & D. Kunzru. (2016). Effect of calcination temperature on stability and activity of Ni/$MgAl_2O_4$ catalyst for steam reforming of methane at high pressure condition. International Journal of Hydrogen Energy, 41(32), 14123–14132.

[19] J. Yoo, S. Park, J. H. Song, S. Yoo, & I. K. Song. (2017). Hydrogen production by steam reforming of natural gas over butyric acid-assisted nickel/alumina catalyst. International Journal of Hydrogen Energy, 42(47), 28377–28385.

[20] I. Iglesias, G. Baronetti, & F. Mariño. (2017). Ni/$Ce_{0.95}M_{0.05}O_2$−δ (M = Zr, Pr, La) for methane steam reforming at mild conditions. International Journal of Hydrogen Energy, 42(50), 29735–29744.

[21] X. Fang, L. Xu, X. Zhang, K. Zhang, H. Dai, W. Liu, ... & W. Zhou. (2019). Effect of rare earth element (Ln = La, Pr, Sm, and Y) on physicochemical properties of the Ni/$Ln_2Ti_2O_7$ catalysts for the steam reforming of methane. Molecular Catalysis, 468, 130–138.

[22] M. Dan, M. Mihet, & M. D. Lazar. (2020). Hydrogen and/or syngas production by combined steam and dry reforming of methane on nickel catalysts. International Journal of Hydrogen Energy, 45(49), 26254–26264.

[23] N. Muradov. (2015). Low-carbon production of hydrogen from fossil fuels. In Compendium of hydrogen energy (pp. 489–522). Woodhead Publishing.

[24] U. I. Amran, A. Ahmad, & M. R. Othman. (2017). Kinetic based simulation of methane steam reforming and water gas shift for hydrogen production using Aspen Plus. Chemical Engineering Transactions, 56, 1681–1686.

[25] G. Di Lullo, A. O. Oni, & A. Kumar. (2021). Blending blue hydrogen with natural gas for direct consumption: Examining the effect of hydrogen concentration on transportation and well-to-combustion greenhouse gas emissions. International Journal of Hydrogen Energy, 46(36), 19202–19216.

[26] E. Meloni, M. Martino, & V. Palma. (2020). A short review on Ni based catalysts and related engineering issues for methane steam reforming. Catalysts, 10(3), 352.

[27] S. T. Wismann, J. S. Engbæk, S. B. Vendelbo, W. L. Eriksen, C. Frandsen, P. M. Mortensen, & I. Chorkendorff. (2019). Electrified methane reforming: Understanding the dynamic interplay. Industrial & Engineering Chemistry Research, 58(51), 23380–23388.

[28] L. Turchetti, M. A. Murmura, G. Monteleone, A. Giaconia, A. A. Lemonidou, S. D. Angeli, ... & M. C. Annesini. (2016). Kinetic assessment of Ni-based catalysts in low-temperature methane/biogas steam reforming. International Journal of Hydrogen Energy, 41(38), 16865–16877.

[29] H. Wu, V. La Parola, G. Pantaleo, F. Puleo, A. M. Venezia, & L. F. Liotta. (2013). Ni-based catalysts for low temperature methane steam reforming: Recent results on Ni-Au and comparison with other bi-metallic systems. Catalysts, 3(2), 563–583.

[30] B. Chu, N. Zhang, X. Zhai, X. Chen, & Y. Cheng. (2014). Improved catalytic performance of Ni catalysts for steam methane reforming in a micro-channel reactor. Journal of Energy Chemistry, 23(5), 593–600.

[31] N. Chanburanasiri, A. M. Ribeiro, A. E. Rodrigues, A. Arpornwichanop, N. Laosiripojana, P. Praserthdam, & S. Assabumrungrat. (2011). Hydrogen production via sorption enhanced steam methane reforming process using Ni/CaO multifunctional catalyst. Industrial & Engineering Chemistry Research, 50(24), 13662–13671.

IZVOD

SIMULACIJA PROCESA I OPTIMIZACIJA PROIZVODNJE VODONIKA IZ PRIRODNOG GASA PUTEM REFORMINGA PARNOG METANA: ISTRAŽIVANJE SIMULACIJE ASPEN HYSYS

Rastuća potražnja za vodonikom u energetskom sektoru zahteva poboljšane metode za njegovu proizvodnju. Trenutno, prirodni gas ostaje primarna sirovina za komercijalnu proizvodnju vodonika. Iako proizvodnja zelenog vodonika iz obnovljivih izvora dobija na pažnji, ona se i dalje suočava sa ekonomskim izazovima u poređenju sa vodonikom dobijenim iz fosilnih goriva. Ova studija se fokusirala na simulaciju proizvodnje vodonika iz prirodnog gasa korišćenjem procesa reforminga parnog metana (SMR). Simulacija je koristila kinetiku Abbas et al (2017) preko 18 tež.% NiO/a-Al_2O_3 katalizatora u okviru Aspen HYSYS V11 softvera i koristila je Peng Robinson paket za fluidne osobine. Sprovedene su analize osetljivosti, sa naglaskom na parametre kao što su temperatura, pritisak, molarna brzina protoka pare i zapremina reaktora. Cilj je bio optimizacija različitih ishoda procesa, uključujući konverziju metana, selektivnost i prinos vodonika, selektivnost i prinos CO, selektivnost i prinos CO_2, odnos H_2/CO i proizvodnju vodonika. Rezultati su pokazali da se konverzija metana i selektivnost za vodonik, ugljen-monoksid i ugljen-dioksid povećavaju sa porastom temperature, a opadaju sa višim pritiskom. Nasuprot tome, konverzija CO i selektivnost metana se smanjuju sa povećanjem temperature, ali se povećavaju sa višim pritiskom. Ovi rezultati su u skladu sa Le Šateljeovim principom i za endotermne i za egzotermne reakcije. Analiza molarnog protoka pare otkrila je povećanu konverziju metana zbog više temperature reakcije koju obezbeđuje para i većeg odnosa pare i ugljenika. Simulacija je pokazala ekonomsku isplativost proizvodnje vodonika kroz proces reforminga parnog metana. Pored toga, istakla je značajan doprinos prodaje pare ukupnoj ekonomskoj isplativosti procesa. Generalno, studija naglašava tehničku izvodljivost proizvodnje vodonika iz prirodnog gasa korišćenjem procesa reforminga parnog metana.

Ključne reči: *Reforming parnog metana, metodologija površine odziva, konverzija CH_4, selektivnost vodonika, simulacija procesa*

Naučni rad
Rad primljen: 11.11.2024.
Rad prihvaćen: 04.01.2025.

Orcid No:
Kenechukwu Conrad Enenebeaku: https://orcid.org/0000-0003-1659-6550
Chritogonus Oudney Akalezi: https://orcid.org/0000-0003-0933-7758
Michael Ogonnaya Ogbuatu: Nil
Stanley Toochukwu Ekwueme: https://orcid.org/0000-0003-3446-0905
Alex Bilar Ali: https://orcid.org/0000-0002-4764-1177
Ijeoma Akunna Duru: https://orcid.org/0000-0002-1427-0816
TochukwuIfeanyi Nwalike: https://orcid.org/0009-0006-0362-0944